Graphene oxide incorporating carbon fibre-reinforced composites submitted to simultaneous impact and fire: Physicochemical characterisation and toxicology of the by-products

Robert Chapple, Carine Chivas-Joly, Ozge Kose, Emmajane Erskine, Laurent Ferry, J. Lopez-Cuesta, Baljinder Kandola, Valérie Forest

Graphene oxide incorporating carbon fibre-reinforced composites submitted to simultaneous impact and fire: Physicochemical characterisation and toxicology of the by-products

Robert Chapple [a], Carine Chivas-Joly [b], Ozge Kose [c], Emmajane L. Erskine [d], Laurent Ferry [e], José-Marie Lopez-Cuesta [e], Baljinder K. Kandola [a,*], Valérie Forest [c,**]

[a] IMRI, University of Bolton, Deane Road, Bolton BL3 5AB, United Kingdom
[b] LNE – Centre for Scientific and Industrial Metrology, CARMEN Plateform, 29, Avenue Roger Hennequin, 78197 Trappes, France
[c] Mines Saint-Etienne, Univ Lyon, Univ Jean Monnet, INSERM, U 1059 Sainbiose, Centre CIS, F-42023 Saint-Etienne, France
[d] DSTL, Porton Down, Salisbury SP4 0JQ, United Kingdom
[e] PCH, IMT Mines Alès, 6 Avenue de Clavières, 30319 Alès Cedex, France

A B S T R A C T

The toxicological profile of particulates released from carbon fibre-reinforced composites (CFC) incorporating nanoadditives, under impact and fire conditions (*e.g.* aircraft crash), is unknown to date. Our aim was to investigate the effects of simultaneous impact and fire on the physicochemical features of the particles released from CFCs produced from a graphene oxide (GO)-reinforced epoxy resin and the consequences on its toxicological profile. CFC samples with (CFC + GO) or without GO (CFC) were subjected to simultaneous impact and fire through a specific setup. Soot and residues were characterised and their toxicity was compared to that of virgin GO. Virgin GO was not cytotoxic but induced pro-inflammatory and oxidative stress responses. The toxicity profile of CFC was similar for soot and residue: globally not cytotoxic, inducing a pro-inflammatory response and no oxidative stress. However, an increased cytotoxicity at the highest concentration was potentially caused by fibres of reduced diameters or fibril bundles, which were observed only in this condition. While the presence of GO in CFC did not alter the cytotoxicity profile, it seemed to drive the pro-inflammatory and oxidative stress response in soot. On the contrary, in CFC + GO residue the biological activity was decreased due to the physicochemical alterations of the materials.

Keywords:
Impact and fire
Toxicity
Carbon fibre-reinforced composites
Nanocomposite
Graphene oxide

1. Introduction

The promising properties of composite materials have resulted in their increasing popularity. Of special interest are carbon fibre-reinforced composites (CFC), which owing to their excellent mechanical properties are used for aerospace, automotive, and many other industrial applications. Carbon based nanoparticle additives, such as nanotubes, graphene or graphene oxides are also increasingly being incorporated in the resin part of the composite to further improve their mechanical properties and provide flame retardancy to the composite (Liu et al., 2012; Xin et al., 2020). These nanoparticles act as a reinforcement at nanoscale. Fire properties can also be improved using these nanoparticle additives as they can act as thermal barriers, reducing the mass loss rate by possibly changing the degradation pathways of the matrix, resulting in a reduced heat release rate and increase in char production (Kandola and Deli, 2014; Katsoulis et al., 2012, 2011; Mouritz and Gibson, 2006; Reis et al., 2014). They can also act as a mass transport barrier to volatile decomposition products, thereby delaying ignition and suppressing combustion (Kandola and Deli, 2014; Katsoulis et al., 2012, 2011).

However, there are concerns regarding the hazards posed by such composite materials in aircraft, or other transport applications, during crash situations (Morrey, 2001). The combination of impact and fire represents a complex situation where decomposed resin, fibres and any incorporated nano or microparticles additives could be released into the surrounding environment. These released particles, fibres or

* Corresponding author.
** Correspondence to: Mines Saint-Etienne, 158 cours Fauriel, CS 62362, 42023 Saint-Etienne Cedex 2, France.
E-mail addresses: B.Kandola@bolton.ac.uk (B.K. Kandola), vforest@emse.fr (V. Forest).

agglomerates, in a size range from many microns to sub-micron, sometimes nano-scale can then remain suspended and transported within smoke. The size distribution, solubility characteristics, and chemical composition of these solid particulates determine their respirability and absorption characteristics, which are the key parameters to the potential physiological effects during human exposure (Gandhi et al., 1999). In situations such as an aeroplane crash, there have been many reports that small fibre pieces can be freed from the main body of the composite, which are sharp enough to puncture human skin, and small enough to be inhaled and carried down the trachea into the lungs (Costantino et al., 2015; Delfa et al., 2009; Gandhi et al., 1999; Hertzberg, 2005). Thus, there is a growing concern regarding the potential health risks for civilians, firefighters and the recovery team, when there is a post-crash fire associated with CFCs (Gandhi, 1999). These concerns are not limited to aerospace as with the increasing popularity of CFCs due to outstanding mechanical properties and reducing costs, many industries, for example automotive, rail, civil structures and sporting equipment are increasing their usage, resultantly increasing the likeliness of unprotected exposure to humans (Reis et al., 2014).

Moreover, the by-products released from a nanocomposite subjected to impact and fire exhibit altered physicochemical features whose characterisation is necessary to fully understand their toxicological profile. Indeed, interactions between nanoparticles and cells, and the subsequent biological outcome, strongly depend on physicochemical features of the nanoparticles. In particular, size, distribution, agglomeration state, shape, crystal structure, chemical composition, surface area, surface chemistry, surface charge, and porosity are of paramount importance (Oberdörster et al., 2005). An international agreement has identified 8 parameters (ISO-TC 229 – ISO/TR 13014:2012) (ISO/TR 13014:2012, 2016) as a minimum to consider for nanotoxicology studies and risk assessment for nanomaterials: i) particle size and particle size distribution, ii) aggregation/ agglomeration state, iii) shape, iv) surface area, v) composition, vi) surface chemistry, vii) surface charge, and viii) solubility/dispersibility (Fadeel et al., 2015). Typically, the biological activity associated with particulates increases as particle size decreases. Nanoparticles with a primary or agglomerate size between 10 and 100 nm will deposit more effectively in the alveolar region than agglomerated particles with sizes between 0.1 and 1 μm. The clearance and translocation of nanoparticles is mainly driven by their geometry and surface characteristics (Braakhuis et al., 2014). Generally, cationic (positively charged) nanoparticles are known to be more cytotoxic than those neutral or anionic (negatively charged) nanoparticles, owing to the fact that cell membranes are anionic and attract cationic nanoparticles (Bussy et al., 2013; Cho et al., 2012). To illustrate the importance of nanoparticle shape, it has been shown that fibre-shaped materials were more toxic to the respiratory system compared to spherical shaped particles of the same chemical composition (Braakhuis et al., 2014).

The aim of this study was to investigate the effects of simultaneous impact and fire on the physicochemical features of the particles released from advanced aerospace and automotive nanocomposites (*i.e.* graphene oxide-reinforced CFC) and the consequences on their toxicological profile. To that purpose, carbon fibre composite from an epoxy resin – graphene oxide nanocomposite (CFC + GO) and an unmodified resin (CFC) were processed through infusion technique. The composite specimens were subjected simultaneously to impact and fire conditions with a specific system previously designed and developed for this purpose with the ability to capture released debris (Chapple et al., 2021). The obtained by-products (soot and residues) were thoroughly characterised, and their *in vitro* toxicity was assessed and compared to that of virgin graphene oxide.

The originality of the present study lies in the fact that we considered the toxicological issues resulting from the simultaneous impact and fire on CFCs containing nano-additives. To the best of our knowledge, this kind of investigation has never been conducted before. Research to date concerning nano-additive release from nanocomposites has been predominantly focused on machining, weathering, washing, contact and incineration (Chivas-Joly et al., 2019, 2016; Froggett et al., 2014) and not on their potential release during simultaneous fire exposure and impact.

2. Materials and methods

2.1. Nanocomposite and carbon fibre-reinforced composites preparation

The epoxy resin (Epilok 60-822 is a diglycidylether of bisphenol A/F resin) and curing agent (Curamine 32-790 NT, an amine-based curing agent) both supplied by Bitrez Ltd, Wigan, UK were mixed in the ratio 100:38 wt% and mechanically stirred for 5 min. Air bubbles were then removed by degassing in a vacuum chamber. Resin was infused into 10 plies of 300 mm × 300 mm carbon fibre fabric by vacuum assisted resin transfer moulding, cured at room temperature for 24 h, followed by post-curing in oven at 80 °C for 8 h, to produce CFC laminates.

Graphene oxide (GO) was sourced from William Blythe, Accrington, UK. This was received as pre-dispersed in epoxy resin at 0.5 wt% and prepared by high shear mixing method. Multiple adaptations to the base CFC resin infusion process were required to produce CFC + GO laminates due to an increased viscosity of the epoxy from the incorporated GO. These laminates were produced on a heated stainless steel base plate to 45 °C, whilst the resin containing GO was heated to 40 °C prior to infusion. During the infusion process a heat gun was required to assist the flow of resin through the fabric plies.

2.2. Exposure of the composites to impact and fire and collection of the by-products (residue and soot)

To achieve a simultaneous impact and fire test, a specific device including a pendulum impactor coupled with a heat source radiant cone was developed (Fig. 1) (Chapple, 2021; Chapple et al., 2021). A short video of the functioning of the system is provided as Supplementary data. This setup also enabled the collection of debris and particles in chambers located at the front face and back face of the system. Additionally, effluents could be sampled from within the extraction system (Fig. 1).

Supplementary material related to this article can be found online at doi:10.1016/j.jhazmat.2021.127544.

Both CFC and CFC + GO samples were subjected simultaneously to impact and fire conditions using this experimental setup. Residual particles and soot were captured during impact and fire (75 kW/m^2) conditions from the back face chamber in an ethanol suspension and from the effluents on a 47 mm diameter polycarbonate filter membrane

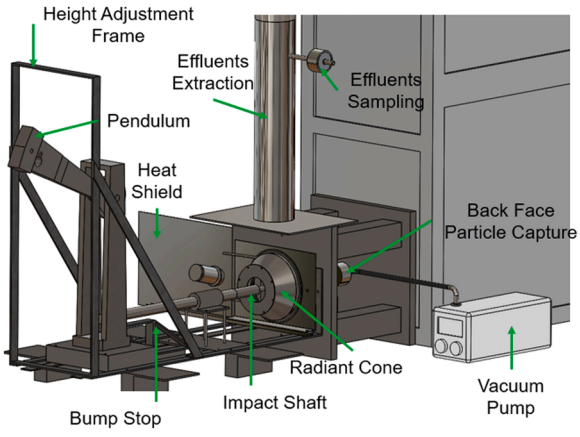

Fig. 1. Bespoke experimental impact and fire equipment set-up developed by Bolton University, IMT Mines Alès and LNE. Reproduced with permission from (Chapple et al., 2021).

(Isopore 0.2 μm GTTP – Merck Millipore) housed in an Advantec LS47, respectively. Several test replicates were required to collect a sufficient total amount (15 mg) of exhaust soot for particle characterisation and the toxicological analysis.

The samples from these two kinds of by-products obtained: soot (collected on the filter) and residues (collected in the back-face chamber) were referred to as: CFC_soot, CFC_residue, CFC + GO_soot, and CFC + GO_residue. A fifth sample consisting of virgin GO alone was used in the toxicological assessments as a reference.

2.3. Physicochemical characterisation of the by-products (soot and residue)

The residual particles and soot from aerosols were characterised using various physicochemical techniques. This task was complex due to numerous parameters to determine (size, surface properties, particles shape, *etc.*). The identification and dimensional measurement of such particles was challenging without prior sample preparation, as it was underlined in the literature (extraction, sonication, surface charge, pH…). Thus, after this first step of sample preparation the dimensional and morphological characterisation were made by Scanning Electron Microscopy (SEM).

2.3.1. Sample preparation for the physicochemical characterisation

The dispersion of particles used in this work was prepared following the procedure described by Ghomrasni et al. (Ghomrasni et al., 2020) and adapted according to the experimental setup, as shown in Fig. 2. Particles collected in residues from the back face were removed from ethanol by centrifuge (Sorvall ST8 Centrifuge with TX-100 Clinical Swinging Bucket) at 4500 RPM for 15 min and concentrated in deionized water (Milli-Q). This sample suspension containing particles was then freeze dried at − 15 °C, to obtain a powder of particles. The powder of particles was then dispersed in ultrapure Milli-Q water to obtain a concentrated suspension for physicochemical characterisations. Next, the suspension of powder was ultrasonicated by Bioblock Scientific Vibracell 75043 probe-sonicator, whilst cooled in by an external ice bath, in order to break down agglomeration and deposited onto a prepared silicon wafer, ready prepared for spin coating (LabSpin 6 SUSS Microtec). Once particles were dispersed across the surface of the wafer, it was then adhered onto an SEM stub ready for analysis. Further details on the preparation of the dispersion can be obtained in our previous works (Delvallée, 2014; Ghomrasni et al., 2020).

To remove particles, predominantly loose soot, from polycarbonate filter membranes, they were initially submerged into Milli-Q water and ultrasonicated whilst cooled by an external ice bath. Once particles were visually observed as removed, filters were carefully removed. This particle suspension was once again sonicated to ensure all agglomerates were broken down and then dispersed across the surface of a silicon wafer, by spin coater, for SEM and Zeta potential characterisation. The remaining suspension was freeze dried as previously described, to achieve particles in powder form, for the potential toxicity study.

2.3.2. Zeta potential measurement

The zeta potential (ZP) measurements were performed using the Malvern Zetasizer Nano ZS. In suspensions, particles are surrounded by a set of ions due to interactions with their charged surface. The zeta potential corresponds to the electrical potential of the layer that remains attached to the particle when this one moves under the action of an electrical field. The optimal dispersion of particles on a substrate depends on zeta potential of the initial suspension. The particles are well dispersed when the suspension is stable and when absolute value of the zeta potential is higher than 30 mV. Fig. 3 shows the evolution of the zeta potential with the pH value for each particle. The change in the zeta potential as a function of pH was carried out by keeping the ionic strength constant with sodium perchlorate solution, perchloric acid and sodium hydroxide of concentration 0.1 mol/L.

The evaluation of the surface charge of particles that promote the adhesion onto the silicon wafer (negative surface charge) shows that virgin GO particles, CFC_soot and CFC + GO_soot samples, exhibited a negative zeta potential, thus a positively charged silicon wafer with poly-L-lysine substrate was required to favour the dispersion. Moreover, CFC_residue and CFC + GO_residue samples, exhibited a positive zeta potential and could be deposited directly onto the negatively charged silicon wafer. Generally, pH could be one factor which can have an influence on the state of aggregation of nanoparticles under different conditions. When pH is equivalent to the isoelectric point pH (pH_{IEP}), particles tend to be agglomerated (Derjaguin and Landau, 1941; Israelachvili, 2011; Verwey, 1947).

2.3.3. SEM measurement

SEM images have been performed with a Zeiss ULTRA-Plus equipped of a Field Emission Gun (FEG) microscope and in-Lens SE detector. All images have been carried out through secondary electrons collected by InLens detector. Size of particles have been determined and this measurand (area-equivalent diameter, $D_{eq.\ area}$), is defined considering that the particles are spherical.

2.4. In vitro toxicity assessment

2.4.1. Samples preparation

The materials derived from the exposure of the composites to impact and fire (soot and residues) were provided as powders that were resuspended in de-ionised water to reach a 1600 μg/mL concentration. Samples were sonicated in ultra-sound bath for 15 min at 130 kHz.

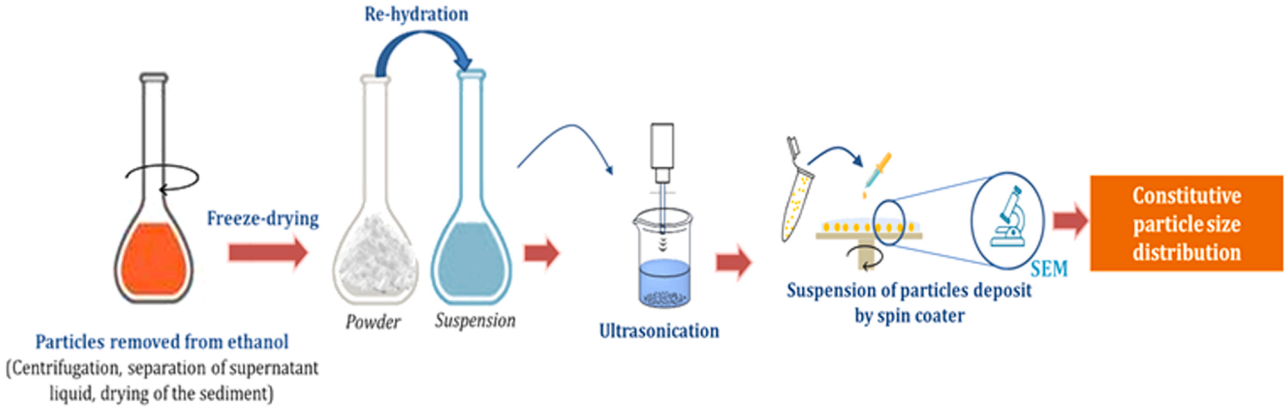

Fig. 2. Sample preparation for physicochemical characterisations adapted from Ghomrasni et al. (2020).

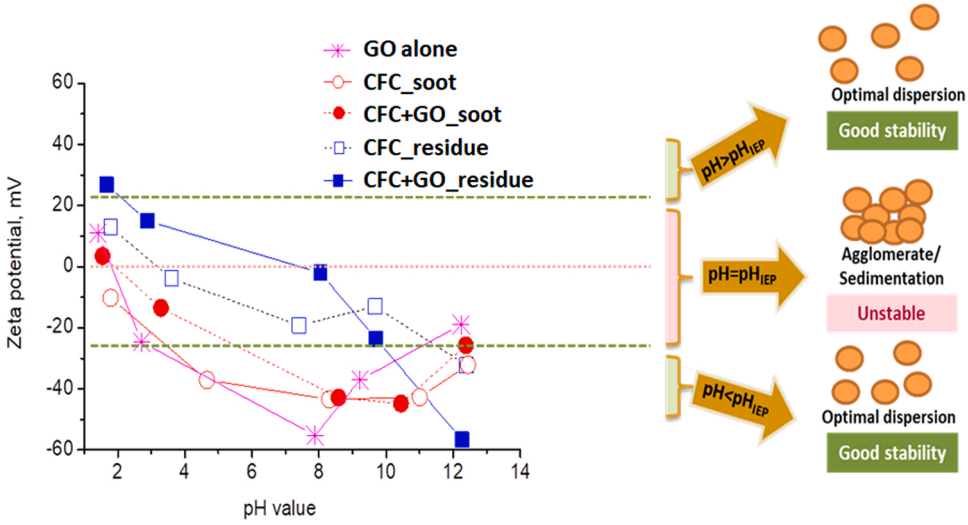

Fig. 3. Zeta potential of the dispersion of the by-products obtained after simultaneous impact and fire, as a function of pH. pH_{IEP}: isoelectric point pH.

2.4.2. Cell culture

The RAW264.7 cell line was used in this study. It derives from mice peritoneal macrophages transformed by the Abelson murine leukaemia virus and was provided by ATCC Cell Biology Collection (Promochem, LGC). The rationale behind the choice of this cellular model is based on the fact that macrophages are ubiquitous cells, part of the immune system and thus they act as the first responders upon exposure to nanomaterials (Drasler et al., 2017; Herd et al., 2015; Palomäki et al., 2015). They are responsible for the recognition and elimination of foreign bodies through phagocytosis. The RAW264.7 cell line is a model widely used in nanotoxicology, especially for the study of inhaled nanomaterials. Cells were cultured in Dulbecco Modified Eagle Medium (DMEM) complemented with 10% of foetal calf serum and 1% of penicillin-streptomycin at 37 °C under a 5% carbon dioxide humidified atmosphere. For contact with the cells, samples were diluted in cell culture medium to reach the following final concentrations: 15, 30, 60 and 120 μg/mL, as recommended for the *in vitro* assessment of nanomaterial hazard (Drasler et al., 2017). Cells were incubated with samples for 24 h before the cell response was assessed.

Contamination of samples with endotoxins was not assessed by specific assays such as the Limulus Amebocyte Lysate (LAL) assay. However, it is quite unlikely as materials were subjected to very high temperatures (700–800 °C) and the toxicological assays were performed in sterile conditions, shortly after the samples were collected (no storage).

2.4.3. Lactate dehydrogenase (LDH) release

For this assay, 25,000 cells were seeded on 96 well plates. Samples were added and incubation lasted for 24 h. To evaluate cell membrane integrity, the cellular release in the supernatant of cytoplasmic lactate dehydrogenase was assessed using the CytoTox-96™ Homogeneous Membrane Integrity Assay (Promega, Charbonnières-les-Bains, France) according to the manufacturer's instructions. The optical density of the samples was determined using a microplate reader (Multiskan RC; Thermolabsystems, Helsinki, Finland) set to 450 nm. Three independent experiments were performed, each in quadruplicate and the activity of the released LDH was reported to that of negative control cells (incubated without nanoparticles). A positive control consisted of the maximal cellular LDH released after cells lysis. To that purpose, cells were incubated with the lysis solution provided by the kit (which is a 9% (weight/volume) solution of Triton X-100 in water) for 45 min at 37 °C.

2.4.4. Pro-inflammatory response

100,000 cells were seeded on 96 well plates. The cells were treated with particle suspensions and after a 24 h exposure, the production of the pro-inflammatory marker Tumour Necrosis Factor alpha (TNF-α) was assessed by the Quantikine® Mouse TNF-α Immunoassay kit (R&D Systems, Lille, France) according to the manufacturer's instructions. The optical density of each sample was determined using a microplate reader (Multiskan RC; Thermolabsystems, Helsinki, Finland) set to 450 nm. Three independent experiments were performed, the production of TNF-α was reported to that of control (unexposed) cells.

As artifacts in the *in vitro* toxicity assays can occur, we previously carried out an extensive study on this topic using carbon-based nanomaterials. Indeed, we assessed the potential artifacts in the LDH release measure (Forest et al., 2015). We concluded that the two main biases observed for this test almost compensated and had no impact on the conclusion. Similarly, we previously assessed interferences that may occur during TNF-α assessment and showed that the TNF-α concentration was slightly underestimated due to a time-dependent degradation and an adsorption on the culture plate wells or on nanoparticles (Pailleux et al., 2013). However, this bias had no significant impact neither on the results of the assays nor on the conclusions. Furthermore, we have considered that the potential artifacts with the carbon-based nanomaterials were limited because the ELISA technique requires numerous washings, therefore the nanomaterials can be considered as eliminated from the medium. Thus, only very limited reaction or adsorption between the nanomaterials and the test reagents could interfere with the colorimetric signal detection.

2.4.5. Determination of reactive oxygen species (ROS) production

100,000 cells were seeded in 96 well black polystyrene microplates and were exposed to the different samples and after 90 min and 24 h of incubation, the level of ROS production was determined using the Oxi-Select™ kit from Cell Bio Labs (San Diego, CA) according to the manufacturer's instructions. Fluorescence was detected using a Fluoroskan Ascent fluorometer (Excitation: 480 nm, Emission: 530 nm, Thermolabsystems), three independent experiments were conducted, and the generation of ROS was reported to that of control (unexposed) cells. A positive control consisting of cells exposed for 90 min or 24 h to 1 mM H_2O_2 was also included in the experiments.

2.4.6. Statistical analyses

Statistical analyses were performed using GraphPad Prism® (version 8.0, GraphPad Software, San Diego, CA, USA). All data were presented as the mean ± the standard deviation (SD). Differences were considered statistically significant when P value was lower than 0.05. One-way Anova Dunnett test analysis was performed for comparison between

control and experimental groups.

3. Results

3.1. Effect of impact and fire on particle release

The SEM observations presented in Fig. 4 showed that particles can exhibit spherical or platelet shapes. The most significant results of the SEM analysis were that GO was observed not only in the residues, which could be expected, but also in the effluents within soot agglomerates. In addition, fibres of reduced diameter were observed in residue.

The size of particles, observed during the SEM analysis, were defined as the equivalent diameter of a sphere to plot the population of the particle size distribution for each sample as presented in Fig. 5. A minimum of 200 measurements were required to have sufficient data to plot the population accurately. Aggregated/agglomerated particles were visible with nano-size constituent particles embedded in the by-products. All measurements have been made on constituent particles that can be easily distinguished through a bounding box to build the histogram of size distribution in aggregates/agglomerates. Graphene oxide sheets have an apparent plate-like structure with multi-layers. The "nano" dimension is difficult to access due to different morphologies or aspect ratios. Therefore it was particularly challenging to establish their size distribution (please see discussion Section 4.1). Particles measured from by-products are mainly coming from the thermal degradation of the matrix. GO seems to be attached to soot agglomerates. The estimation of the law parameters that best fits the SEM data was carried out using R-Studio software with a programme developed by the LNE statistics team.

Table 1 summarises the statistical parameters from SEM measurement – (mean, modal and median diameters), D_{modal} is the average size of the most frequented class, D_{median} is the size that splits the distribution into two equal parts of areas. For all the samples, the distributions were fitted with a log normal law.

3.2. In vitro toxicity assessment of the by-products

3.2.1. Cytotoxicity

The results of the LDH release assay, corresponding to cell membrane damage and thus the cytotoxicity induced, are reported in Fig. 6.

Only the highest dose (120 μg/mL) of CFC_residue sample triggered a cytotoxicity significantly different from that observed in control cells (unexposed to nanoparticles). The other samples did not induce cytotoxicity.

3.2.2. Pro-inflammatory response

The results of the production of TNF-α, a major pro-inflammatory cytokine, are reported in Fig. 7.

CFC + GO_residue did not induce a pro-inflammatory response while all the other samples did. This response was dose-dependent. CFC_soot triggered a pro-inflammatory response that was significantly different from that of control cells at the highest doses (from 60 μg/mL). The highest pro-inflammatory effects were observed when cells were incubated with GO alone and CFC + GO_soot.

3.2.3. Reactive oxygen species (ROS) production

The results of the production of ROS, indicative of the induction of oxidative stress, are reported in Fig. 8.

After 90 min of cell-sample contact, only GO alone (from the 30 μg/mL concentration) triggered a production of ROS significantly higher than that observed in control (unexposed) cells. All the other samples did not induce an increased ROS production.

After 24 h of cell-sample contact, GO alone exhibited a significantly enhanced ROS production compared to control cells. This production increased with particle concentration. Similarly, CFC + GO_soot induced a ROS production in a concentration-dependent manner, although it was significantly different from that of control cells only from 30 μg/mL.

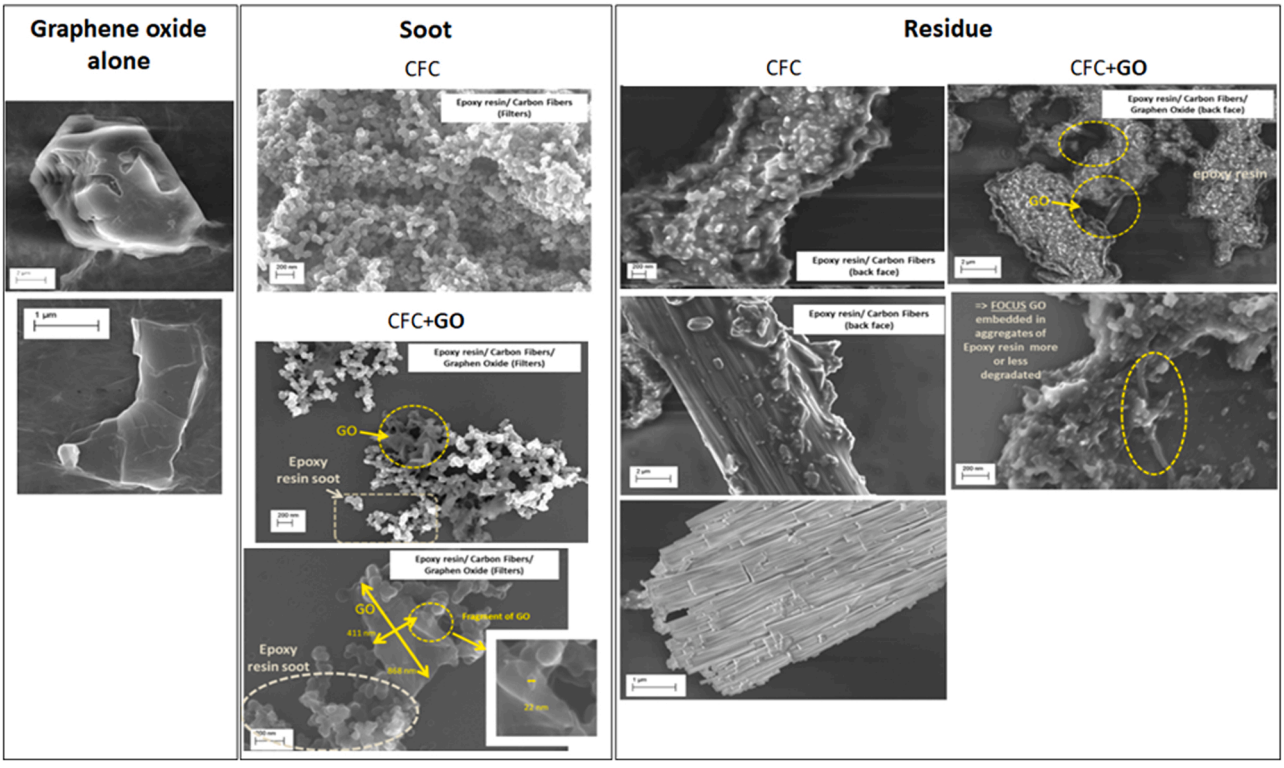

Fig. 4. Morphology of soot and residues coming from pristine GO, CFC and CFC + GO samples subjected to simultaneous impact and fire and deposited on silica substrate.

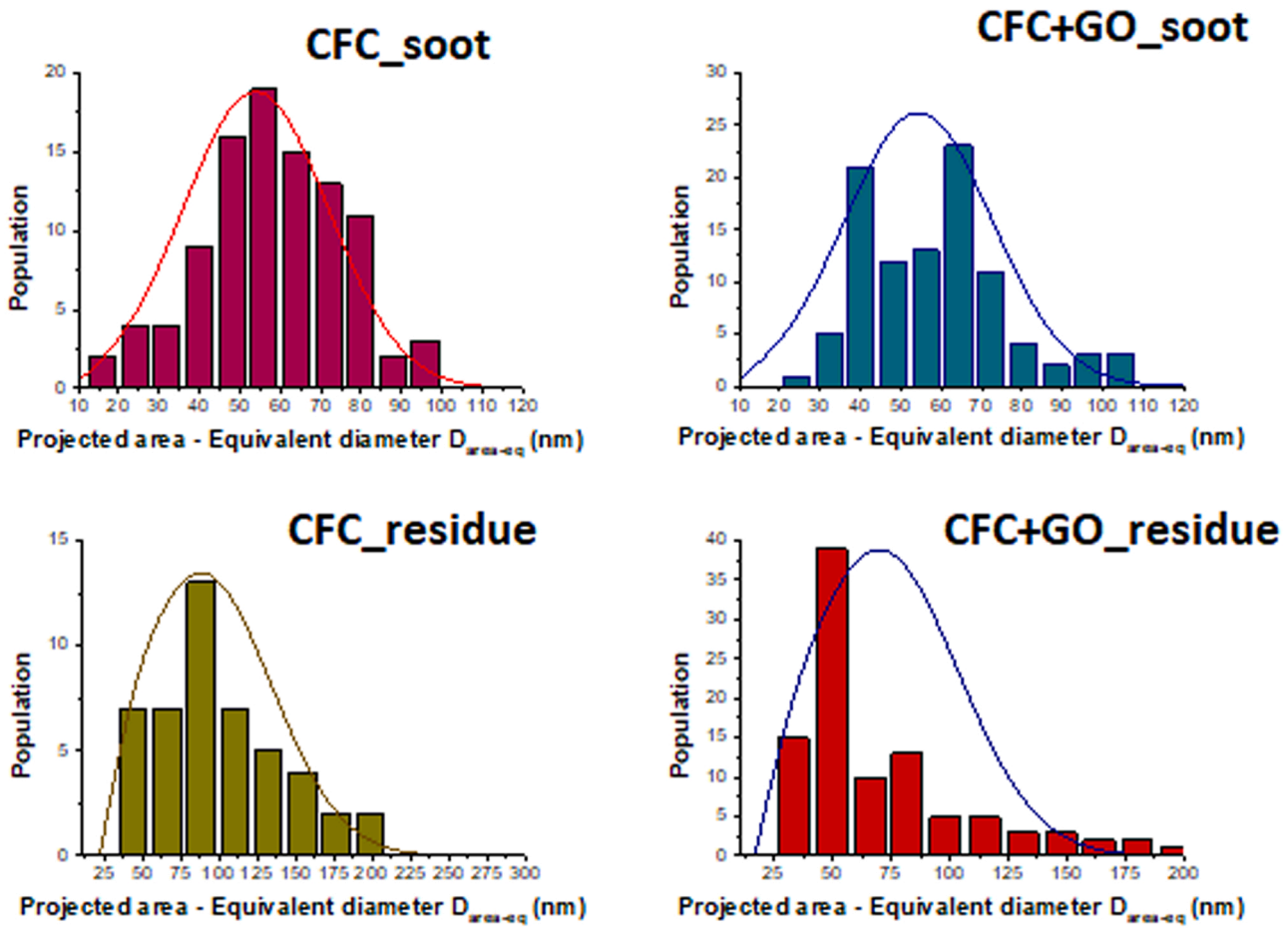

Fig. 5. Size distribution of by-products (soot and residue) coming from CFC and CFC + GO samples after impact and fire.

Table 1
Statistical parameters from SEM measurement – (mean, modal and median diameters), D_{modal} is the average size of the most frequented class, D_{median} is the size that splits the distribution into two equal parts of areas.

Sample	Measurement			
	$D_{SEM\ mean\ area\text{-}eq}$ (nm)	Standard deviation of the size distribution	D_{Modal} (nm)	D_{Median} (nm)
CFC_soot	54.4	21.3	43.9	50.7
CFC_residue	88.1	44.1	63.0	78.8
CFC + GO_soot	54.4	18.8	45.9	51.4
CFC+GO_residue	44.2	20.6	32.9	40.1

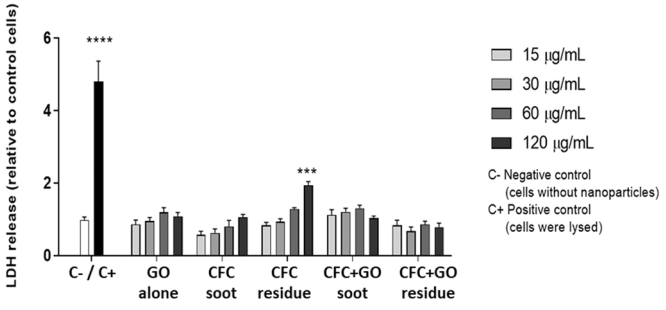

Fig. 6. Cytotoxicity of the 5 samples as determined by the LDH release. Results are expressed relative to control (unexposed cells). Statistically different from control cells ****$p < 0.0001$, ***$p < 0.001$.

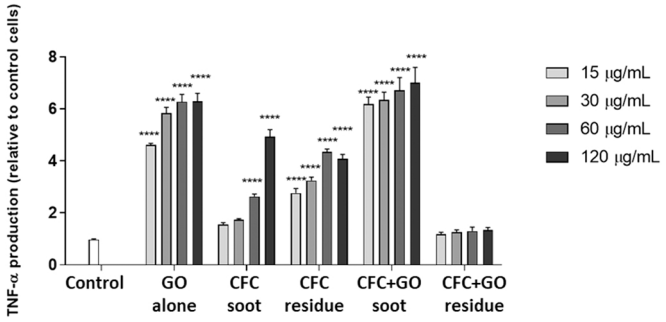

Fig. 7. Pro-inflammatory response induced by the 5 samples as determined by the production of TNF-α. Results are expressed relative to control (unexposed) cells. Statistically different from control cells ****$p < 0.0001$.

4. Discussion

4.1. Challenges to determine size distribution with mixture of fibres and particles

The by-products (soot and residue) studied coming from the combination of impact and fire were polydispersed particle mixtures with different shapes and of a broad size distribution. The mean size diameter evaluated corresponded to the diameter estimated from a projected surface area.

For CFC, images from SEM analysis and results from zeta potential measurements indicate similar behaviour with a mean equivalent diameter close to 54.4 nm and an isoelectric point (noted IEP) around

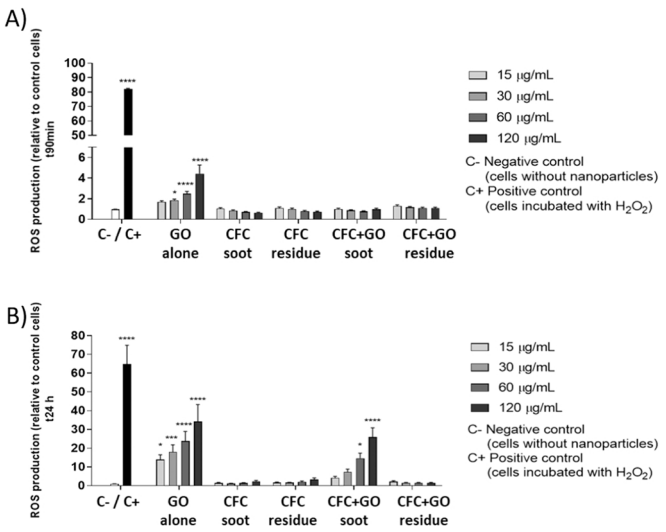

Fig. 8. Oxidative stress induced by the 5 samples as determined by the production of ROS after 90 min (A) and 24 h (B) of cell-sample contact. Results are expressed relative to control (unexposed) cells. Statistically different from control cells ****$p < 0.0001$, ***$p < 0.001$, *$p < 0.05$.

1–2, whether or not graphene oxide was present (see Fig. 3). The zeta potential was measured to analyse the surface charge and the agglomeration state of particles. When the zeta-potential is equal to zero, the agglomeration will be maximum, and all agglomerates will be formed. It was noticed that the zeta potential for soot by-products was not affected by the presence of graphene oxide and the evolution of the curve of zeta potential was close to the pristine GO nanoparticles.

Even if residual by-products from CFC + GO present some similar shaped nanoparticles to CFC (Fig. 4), the presence of GO has an impact on constituent nanoparticle size in the residue. The mean equivalent diameter measured for residual by-products decreased for CFC with graphene oxide. The state of agglomeration/aggregation depends on the zeta potential and the pH (Gao et al., 2008).

In our case, the zeta potential value increased with graphene oxide in the residual by-products, and exhibited a zeta potential close to −60 mV at basic pH. Zeta potential measurements in presence of graphene oxide induced a diminution of the aggregation. The fate of by-products (soot and residue) from CFC highlights the important role of the graphene oxide on the released particles during the simultaneous impact and fire. Carbon fibrils and fibres from by-products were measured with a mean diameter evaluated at < 1 µm and 11.2 ± 4.2 µm, respectively.

4.2. Toxicological profile of the by-products released after simultaneous exposure to impact and fire of the nanocomposite

The toxicity profiles of the 5 samples are compared in the summarising Table 2.

GO alone was not cytotoxic but was able to induce pro-inflammatory effects and oxidative stress. The toxicity profile of CFC was similar for soot and residue: globally not cytotoxic (except at the highest concentration for residue), inducing a pro-inflammatory response and no oxidative stress. While the presence of GO in CFC did not alter the cytotoxicity profile (both for soot and residue), it had a significant impact on the pro-inflammatory response and oxidative stress. Indeed, with GO in the CFC, the pro-inflammatory response was increased in soot and decreased in residue, whereas the oxidative stress was also increased in soot after 24 h, but there was no impact on residue.

These toxicological profiles should be analysed with regard to the physicochemical features of the samples as it has been shown that they are closely correlated with the toxicity induced (Oberdörster et al., 2005). Regarding cytotoxicity (Fig. 6), only particles from the CFC_residue sample exhibited a response significantly different from that observed in control (unexposed) cells at the highest dose (120 µg/mL). Interestingly, in this sample individual fibrils were observed (Fig. 4). The individual fibrils, within fibril bundles, had diameters less than 1 µm and lengths in the range 5–20 µm. It has been reported that fibres with diameters less than 3 µm and lengths between 3 and 10 µm can penetrate macrophage cell membranes (Gandhi, 1999; Hoet et al., 2004; Morrey, 2001), causing cell membranes damage, potentially explaining this observed cytotoxicity.

The addition of GO in the CFC + GO samples provided flame retardancy mechanisms (Liu et al., 2012; Yin et al., 1994). Thus, fibres were better protected during decomposition, compared to CFC samples and fibrils bundles were not observed, providing an explanation for the absence of cytotoxicity of CFC + GO_residue compared to epoxy CFC_residue.

Similarly, the absence of fibrils in the CFC + GO_residue could explain the absence of a pro-inflammatory response, unlike what was observed with the other samples (Fig. 7). Indeed, due to their shape and dimensions, fibrils cannot be fully internalised by macrophages, inducing the so-called frustrated phagocytosis. This results in the continuous stimulation of the immune system by the release of pro-inflammatory cytokines such as TNF-α (Møller et al., 2014; Padmore et al., 2017; Schinwald et al., 2012).

Regarding oxidative stress, GO alone triggered a production of ROS significantly higher than that observed in control cells (90 min and 24 h) as well as CFC + GO_soot at 24 h for the highest concentrations (Fig. 6). As it was observed that GO was attached to soot agglomerates (Fig. 4) captured from the effluents of the CFC + GO_soot sample, it can be concluded that GO is responsible for triggering the production of ROS. Potentially, the morphology and/or the surface chemistry of GO may cause disruption to the cells, damaging macromolecules, such as proteins, DNA and lipids. This affects cell metabolism and signalling, resulting in excessive ROS generation, which is the first stage of the mechanisms related to carcinogenesis, ageing, and mutagenesis (Jarosz et al., 2016).

Toxicological studies performed on carbon fibres have reported no major health concerns and have been performed at dosage levels and exposure times much higher than those encountered during fire exposure, suggesting there is no acute lung injury and other long-term respiratory problems associated with the inhalation of carbon fibres (Owen et al., 1986; Thomson et al., 1990; Warheit et al., 1994; Waritz et al., 1998). However, during burning conditions, the fibres released from composites may be substantially different considering their potential contamination with various chemicals and combustion products from the polymer matrix. Thus, contaminated fibres may pose different toxicological properties to virgin carbon fibres (Mouritz and Gibson, 2006). The fibres may also reduce in diameter during fire exposure, due to oxidation and fibrillation. The diameter of typical virgin carbon fibres ranges between 5 and 7.5 µm and analysis of fibres collected from burning carbon fibre epoxy composites reported fibre diameter range between 1.5 and 7.5 µm. Approximately 60% of those fibres were small enough to be inhaled deep into the lungs (Mouritz and Gibson, 2006). This is consistent with our measurements (mean fibre diameter 11.2 ± 4.2 µm and fibril diameters less than 1 µm).

In addition, nanoparticle additives are commonly included in composites to improve their mechanical and/or flammability properties, providing another potential source of hazard. As discussed before, the biological activity of nanoparticles is dependent on their physicochemical parameters (Oberdörster et al., 2005). It is thus of paramount importance to characterise the by-products as the impact and fire can significantly alter their features. For instance, GO was observed not only

Table 2
Comparison of the morphology and toxicological profile of the 5 samples.

	GO alone	CFC		CFC + GO	
		Soot	Residue	Soot	Residue
SEM picture					
Cytotoxicity	–	–	- (+ only at the highest dose)	–	–
Pro-inflammatory response	+++	++	++	+++	–
Oxidative stress 90 min	+	–	–	–	–
Oxidative stress 24 h	++	–	–	++	–

in the residues, which could be expected, but also in the soot. This demonstrates that it can be released from the sample and remain airborne. We focused our research on GO because of its growing interest in composites sector and less knowledge of its toxicity while in usage. However, other nanofillers exist such as carbon nanotubes, montmorillonite clay or layered double hydroxide clays and it should be of interest to extend such research to them.

To the best of our knowledge, no information is available in the literature on the effects of simultaneous impact and fire on carbon fibre-reinforced polymer containing nano-additives making it difficult to compare our results. However, data has been reported on the separate effects of impact or fire. As an example, Chivas-Joly et al. compared the *in vitro* cytotoxicity induced by pristine nanofillers, to that triggered by soot and residual ash obtained after incineration of Al-based nanocomposites. They clearly observed that the residual ash of Al-based nanocomposites was not cytotoxic, unlike soot, and showed that safe pristine boehmite nanoparticles became toxic due to a chemical modification after the incineration process. It was concluded that the physicochemical features of nanoparticles can be modified by the incineration process and the available toxicological data on pristine nanofillers might not be relevant to assess the modified nanoparticles included in soot (Chivas-Joly et al., 2019). These results, although obtained with different materials and a different experimental setup are in good agreement with the results of the present study.

Risk assessment involves the evaluation of the contribution of two factors: hazard and exposure. Here we described the toxicological profiles of the by-products obtained after materials were submitted to simultaneous impact and fire. It should be interesting to complete this study by the assessment of the human exposure to soot and residue respectively. As previously mentioned, during a crash, humans can be exposed mainly through inhalation (Costantino et al., 2015; Delfa et al., 2009; Gandhi et al., 1999; Hertzberg, 2005). Nevertheless, residue and soot can also deposit back onto land leading to soil contamination. Through diffusion in soil or water compartments, humans can be indirectly exposed (through food, water…), as well as the ecosystem. Therefore, our findings could also be interesting for the ecotoxicology field.

5. Conclusion

Fig. 9 proposes a schematic summary of our findings.

Simultaneous impact and fire conditions were applied to a carbon fibres-reinforced composite with and without graphene oxide as a nano-additive. Virgin GO alone was not cytotoxic but did induce pro-inflammatory and oxidative stress responses. The toxicity profile of CFC was similar in soot and residue: globally not cytotoxic (except at the highest concentration for residue), inducing a pro-inflammatory response and no oxidative stress. The increased cytotoxicity at the highest concentration was potentially caused by fibres of reduced diameters or fibril bundles, which were observed only in this condition. While the presence of GO in CFC + GO did not alter the cytotoxicity profile (both for soot and residue), it seems to drive the pro-inflammatory and oxidative stress (after 24 h) response in soot. On the contrary, for residue the biological activity was decreased due to the physicochemical alterations of the materials.

Taken together, our results call for caution and argue for the fact that the toxicological profile of a nanocomposite submitted to impact and fire conditions cannot be extrapolated from the toxicological profile of its components. For a better risk management, it would now be interesting to perform further analyses on the level of human exposure to residue and soot.

Funding

This work was supported by Dstl, UK.

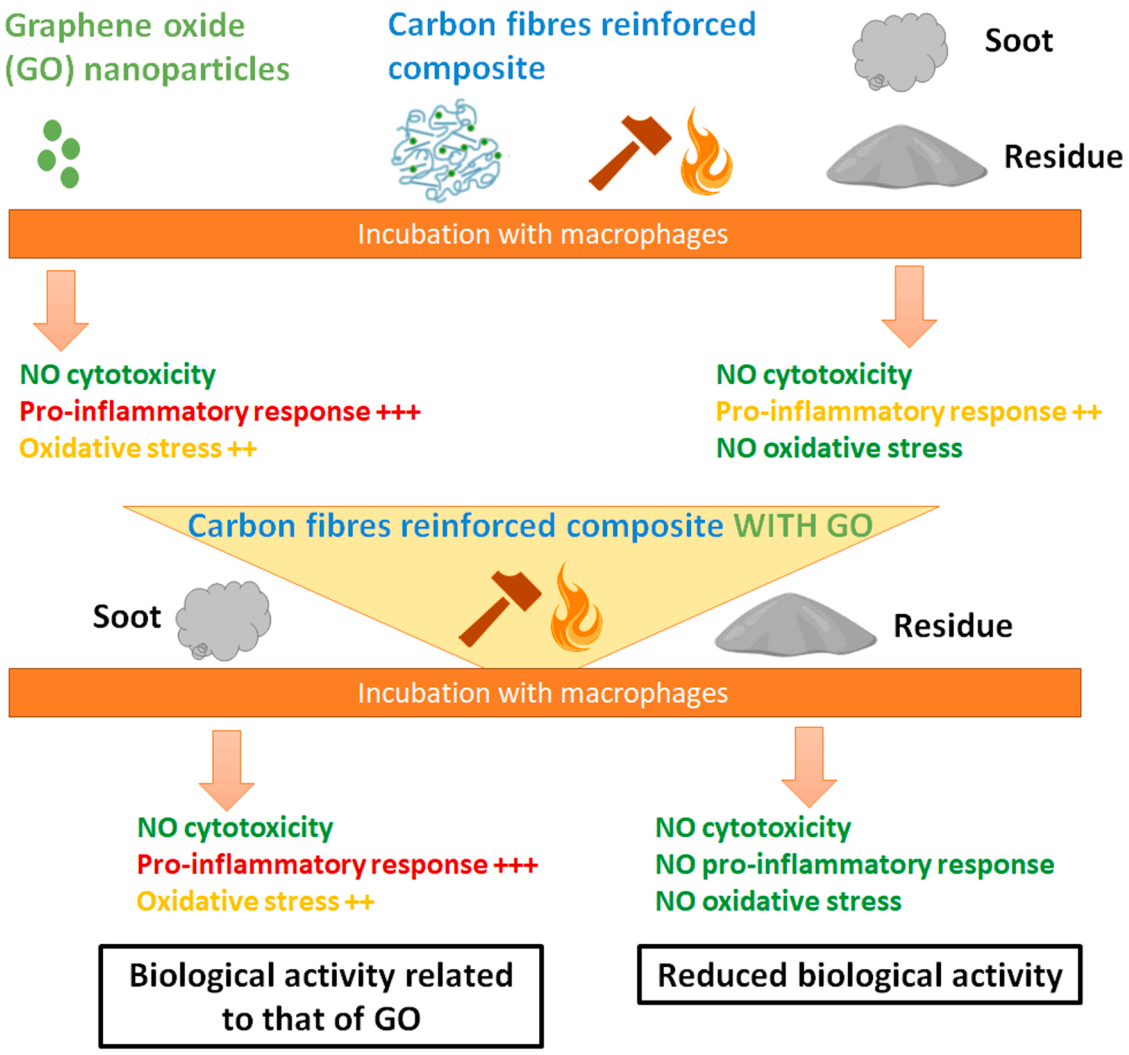

Fig. 9. Schematic summary of the main results of this study.

CRediT authorship contribution statement

Robert Chapple: Conceptualization, Investigation, Writing – original draft. **Carine Chivas-Joly:** Conceptualization, Investigation, Supervision, Writing – original draft. **Ozge Kose:** Investigation. **Emmajane L. Erskine:** Conceptualization, Funding acquisition, Writing – review & editing. **Laurent Ferry:** Conceptualization, Supervision, Writing – review & editing. **José-Marie Lopez-Cuesta:** Conceptualization, Supervision, Writing – review & editing. **Baljinder K. Kandola:** Conceptualization, Project administration, Supervision, Writing – review & editing. **Valérie Forest:** Conceptualization, Supervision, Writing – original draft.

Declaration of Competing Interest

The authors declare that they have no known competing financial interests or personal relationships that could have appeared to influence the work reported in this paper.

Acknowledgements

The authors acknowledge the Dstl, UK for the financial and technical assistance; Bitrez Ltd. UK for supply of the resin; and William Blythe, UK for supply and dispersion of GO. Authors also thank J. Milnes from University of Bolton; L. Dumazert, R. Ravel and J-C. Roux from IMT Ales; and F. De Lagos from Fire Department at LNE, for their technical support.

References

Braakhuis, H.M., Park, M.V., Gosens, I., De Jong, W.H., Cassee, F.R., 2014. Physicochemical characteristics of nanomaterials that affect pulmonary inflammation. Part. Fibre Toxicol. 11, 18. https://doi.org/10.1186/1743-8977-11-18.

Bussy, C., Ali-Boucetta, H., Kostarelos, K., 2013. Safety considerations for graphene: lessons learnt from carbon nanotubes. Acc. Chem. Res. 46, 692–701. https://doi.org/10.1021/ar300199e.

Chapple, R., 2021. Effect of Simultaneous Impact and Heat/fire on Carbon Fibre-Reinforced Composites Containing Nano Additives. University of Bolton, UK.

Chapple, R., Kandola, B.K., Myler, P., Ferry, L., Lopez-Cuesta, J.-M., Chivas-Joly, C., Erskine, E.L., 2021. The effect of simultaneous heat/fire and impact on carbon fibril and particle release from carbon fibre-reinforced composites. Polym. Compos. https://doi.org/10.1002/pc.26290.

Chivas-Joly, C., Gaie-Levrel, F., Motzkus, C., Ducourtieux, S., Delvallée, A., De Lagos, F., Nevé, S.L., Gutierrez, J., Lopez-Cuesta, J.-M., 2016. Characterization of aerosols and fibers emitted from composite materials combustion. J. Hazard. Mater. 301, 153–162. https://doi.org/10.1016/j.jhazmat.2015.08.043.

Chivas-Joly, C., Longuet, C., Pourchez, J., Leclerc, L., Sarry, G., Lopez-Cuesta, J.-M., 2019. Physical, morphological and chemical modification of Al-based nanofillers in by-products of incinerated nanocomposites and related biological outcome. J. Hazard. Mater. 365, 405–412. https://doi.org/10.1016/j.jhazmat.2018.10.029.

Cho, W.-S., Duffin, R., Thielbeer, F., Bradley, M., Megson, I.L., MacNee, W., Poland, C.A., Tran, C.L., Donaldson, K., 2012. Zeta potential and solubility to toxic ions as mechanisms of lung inflammation caused by metal/metal oxide nanoparticles. Toxicol. Sci. 126, 469–477. https://doi.org/10.1093/toxsci/kfs006.

Costantino, J., Jarbeau, J., Hintz, T., Hinojosa, M., 2015. Composite Material Hazard Assessment at Crash Sites Composite Material Hazard Assessment at Crash Sites –

[PDF Document] [WWW Document]. fdocuments.in. URL: ⟨https://fdocuments.in/document/composite-material-hazard-assessment-at-crash-sites-composite-material-hazard-assessment.html⟩. (Accessed 17 May 2021).
Delfa, G.L., Luinge, J.W., Gibson, A.G., 2009. Integrity of composite aircraft fuselage materials under crash fire conditions. Plast. Rubber Compos. 38, 111–117. https://doi.org/10.1179/174328909×387900.
Delvallée, A., 2014. Métrologie dimensionnelle de nanoparticules mesurées par AFM et par MEB (These de doctorat). École nationale supérieure de techniques avancées, Palaiseau.
Derjaguin, B., Landau, L., 1941. Theory of the stability of strongly charged lyophobic sols and of the adhesion of strongly charged particles in solutions of electrolytes. Acta Physicochim. URSS 14, 633.
Drasler, B., Sayre, P., Steinhäuser, K.G., Petri-Fink, A., Rothen-Rutishauser, B., 2017. In vitro approaches to assess the hazard of nanomaterials. NanoImpact 8, 99–116. https://doi.org/10.1016/j.impact.2017.08.002.
Fadeel, B., Fornara, A., Toprak, M.S., Bhattacharya, K., 2015. Keeping it real: the importance of material characterization in nanotoxicology. Biochem. Biophys. Res. Commun. Nanomed. 468, 498–503. https://doi.org/10.1016/j.bbrc.2015.06.178.
Forest, V., Figarol, A., Boudard, D., Cottier, M., Grosseau, P., Pourchez, J., 2015. Adsorption of lactate dehydrogenase enzyme on carbon nanotubes: how to get accurate results for the cytotoxicity of these nanomaterials. Langmuir 31, 3635–3643. https://doi.org/10.1021/acs.langmuir.5b00631.
Froggett, S.J., Clancy, S.F., Boverhof, D.R., Canady, R.A., 2014. A review and perspective of existing research on the release of nanomaterials from solid nanocomposites. Part. Fibre Toxicol. 11, 17. https://doi.org/10.1186/1743-8977-11-17.
Gandhi, S., 1999. Postcrash health hazards from burning aircraft composites. Aviat. Fire J. 6.
Gandhi, S., Lyon, R., Speitel, L., 1999. Potential health hazards from burning aircraft composites. J. Fire Sci. 17, 20–41. https://doi.org/10.1177/073490419901700102.
Gao, J., Bonzongo, J.-C.J., Bitton, G., Li, Y., Wu, C.-Y., 2008. Nanowastes and the environment: using mercury as an example pollutant to assess the environmental fate of chemicals adsorbed onto manufactured nanomaterials. Environ. Toxicol. Chem. 27, 808–810. https://doi.org/10.1897/07-282.1.
Ghomrasni, N.B., Chivas-Joly, C., Devoille, L., Hochepied, J.-F., Feltin, N., 2020. Challenges in sample preparation for measuring nanoparticles size by scanning electron microscopy from suspensions, powder form and complex media. Powder Technol. 359, 226–237. https://doi.org/10.1016/j.powtec.2019.10.022.
Herd, H.L., Bartlett, K.T., Gustafson, J.A., McGill, L.D., Ghandehari, H., 2015. Macrophage silica nanoparticle response is phenotypically dependent. Biomaterials 53, 574–582. https://doi.org/10.1016/j.biomaterials.2015.02.070.
Hertzberg, T., 2005. Dangers relating to fires in carbon-fibre based composite material. Fire Mater. 29, 231–248. https://doi.org/10.1002/fam.882.
Hoet, P.H., Brüske-Hohlfeld, I., Salata, O.V., 2004. Nanoparticles – known and unknown health risks. J. Nanobiotechnol. 2, 12. https://doi.org/10.1186/1477-3155-2-12.
ISO/TR 13014:2012, 2016. Nanotechnologies – Guidance on Physico-Chemical Characterization of Engineered Nanoscale Materials for Toxicologic Assessment [WWW Document]. ISO. URL: ⟨http://www.iso.org/iso/catalogue_detail?csnumber=52334⟩. (Accessed 28 November 2016).
Israelachvili, J.N., 2011. Intermolecular and Surface Forces, 3rd ed. Elsevier Science.
Jarosz, A., Skoda, M., Dudek, I., Szukiewicz, D., 2016. Oxidative stress and mitochondrial activation as the main mechanisms underlying graphene toxicity against human cancer cells. Oxid. Med. Cell. Longev. 2016, 5851035 https://doi.org/10.1155/2016/5851035.
Kandola, B.K., Deli, D., 2014. Chapter 16 – flame-retardant thermoset nanocomposites for engineering applications. In: Papaspyrides, C.D., Kiliaris, P. (Eds.), Polymer Green Flame Retardants. Elsevier, Amsterdam, pp. 503–549. https://doi.org/10.1016/B978-0-444-53808-6.00016-0.
Katsoulis, C., Kandare, E., Kandola, B.K., 2011. The effect of nanoparticles on structural morphology, thermal and flammability properties of two epoxy resins with different functionalities. Polym. Degrad. Stab. 96, 529–540. https://doi.org/10.1016/j.polymdegradstab.2011.01.002.
Katsoulis, C., Kandola, B.K., Myler, P., Kandare, E., 2012. Post-fire flexural performance of epoxy-nanocomposite matrix glass fibre composites containing conventional flame retardants. Compos. Part Appl. Sci. Manuf. 43, 1389–1399. https://doi.org/10.1016/j.compositesa.2012.03.009.
Liu, Q., Zhou, X., Fan, X., Zhu, C., Yao, X., Liu, Z., 2012. Mechanical and thermal properties of epoxy resin nanocomposites reinforced with graphene oxide. Polym. Plast. Technol. Eng. 51, 251–256. https://doi.org/10.1080/03602559.2011.625381.
Møller, P., Christophersen, D.V., Jensen, D.M., Kermanizadeh, A., Roursgaard, M., Jacobsen, N.R., Hemmingsen, J.G., Danielsen, P.H., Cao, Y., Jantzen, K., Klingberg, H., Hersoug, L.-G., Loft, S., 2014. Role of oxidative stress in carbon nanotube-generated health effects. Arch. Toxicol. 88, 1939–1964. https://doi.org/10.1007/s00204-014-1356-x.
Morrey, E.L., 2001. Potential Hazards Associated with Combustion of Polymer Composite Materials and Strategies for their Mitigation (Ph.D. thesis). Imperial College London (University of London).
Mouritz, A.P., Gibson, A.G., 2006. Fire Properties of Polymer Composite Materials, Solid Mechanics and Its Applications. Springer, Netherlands. https://doi.org/10.1007/978-1-4020-5356-6.
Oberdörster, G., Maynard, A., Donaldson, K., Castranova, V., Fitzpatrick, J., Ausman, K., Carter, J., Karn, B., Kreyling, W., Lai, D., Olin, S., Monteiro-Riviere, N., Warheit, D., Yang, H., 2005. A report from the ILSI Research Foundation/Risk Science Institute Nanomaterial Toxicity Screening Working Group, principles for characterizing the potential human health effects from exposure to nanomaterials: elements of a screening strategy. Part. Fibre Toxicol. 2, 8. https://doi.org/10.1186/1743-8977-2-8.
Owen, P.E., Glaister, J.R., Ballantyne, B., Clary, J.J., 1986. Subchronic inhalation toxicology of carbon fibers. J. Occup. Med. Publ. Ind. Med. Assoc. 28, 373–376.
Padmore, T., Stark, C., Turkevich, L.A., Champion, J.A., 2017. Quantitative analysis of the role of fiber length on phagocytosis and inflammatory response by alveolar macrophages. Biochim. Biophys. Acta Gen. Subj. 1861, 58–67. https://doi.org/10.1016/j.bbagen.2016.09.031.
Pailleux, M., Boudard, D., Pourchez, J., Forest, V., Grosseau, P., Cottier, M., 2013. New insight into artifactual phenomena during in vitro toxicity assessment of engineered nanoparticles: study of TNF-α adsorption on alumina oxide nanoparticle. Toxicol. Vitr. 27, 1049–1056. https://doi.org/10.1016/j.tiv.2013.01.022.
Palomäki, J., Sund, J., Vippola, M., Kinaret, P., Greco, D., Savolainen, K., Puustinen, A., Alenius, H., 2015. A secretomics analysis reveals major differences in the macrophage responses towards different types of carbon nanotubes. Nanotoxicology 9, 719–728. https://doi.org/10.3109/17435390.2014.969346.
Reis, P., Ferreira, J.A.M., Zhang, Z.Y., Benameur, T., Richardson, M., 2014. Impact strength of composites with nano-enhanced resin after fire exposure. Compos. Part B Eng. 56, 290–295. https://doi.org/10.1016/j.compositesb.2013.08.048.
Schinwald, A., Murphy, F.A., Jones, A., MacNee, W., Donaldson, K., 2012. Graphene-based nanoplatelets: a new risk to the respiratory system as a consequence of their unusual aerodynamic properties. ACS Nano 6, 736–746. https://doi.org/10.1021/nn204229f.
Thomson, S.A., Hilaski, R.J., Wright, R., Mattie, D., 1990. Nonrespirability of Carbon Fibers in Rats from Repeated Inhalation Exposure. Final Report, July–November 1989 (No. AD-A-228196/2/XAB; CRDEC-TR-149). Chemical Research, Development and Engineering Center, Aberdeen Proving Ground, MD (USA).
Verwey, E.J.W., 1947. Theory of the stability of lyophobic colloids. J. Phys. Colloid Chem. 51, 631–636. https://doi.org/10.1021/j150453a001.
Warheit, D.B., Hansen, J.F., Carakostas, M.C., Hartsky, M.A., 1994. Acute inhalation toxicity studies in rats with a respirable-sized experimental carbon fibre: pulmonary biochemical and cellular effects. Ann. Occup. Hyg. 38, 769–776. https://doi.org/10.1093/annhyg/38.inhaled_particles_VII.769.
Waritz, R.S., Ballantyne, B., Clary, J.J., 1998. Subchronic inhalation toxicity of 3.5-μm diameter carbon fibers in rats. J. Appl. Toxicol. 18, 215–223. https://doi.org/10.1002/(SICI)1099-1263(199805/06)18:3<215::AID-JAT499>3.0.CO;2-W.
Xin, W., Sarasini, F., Tirillò, J., Bavasso, I., Sbardella, F., Lampani, L., De Rosa, I.M., 2020. Impact and post-impact properties of multiscale carbon fiber composites interleaved with carbon nanotube sheets. Compos. Part B Eng. 183, 107711 https://doi.org/10.1016/j.compositesb.2019.107711.
Yin, Y., Binner, J.G.P., Cross, T.E., Marshall, S.J., 1994. The oxidation behaviour of carbon fibres. J. Mater. Sci. 29, 2250–2254. https://doi.org/10.1007/BF01154706.